

THE EFFECT OF THE IMPRINTED SILICAS PREPARED BY SOL-GEL ROUTE ON ADSORPTION OF RHODAMINE B: TEXTURAL AND STRUCTURAL ASPECTS

C. E. Escobar¹; J. H. Z. dos Santos²

- 1- Departamento de Engenharia Química – Universidade Federal do Rio Grande do Sul
Rua Eng. Luis Englert s/n – CEP: 90040-040 – Porto Alegre - RS – Brasil – Email: cicero.escobar@gmail.com
- 2- Instituto de Química - Universidade Federal do Rio Grande do Sul
Av. Bento Gonçalves 9500 - CEP: 91500-000 - Porto Alegre – RS - Brasil.
Telefone: (51) 3316 7238– Fax: (51) 3316 730 4– Email: jhzds@iq.ufrgs.br

ABSTRACT: A series of silica xerogels, bearing Rhodamine B as the template were synthesized by distinct sol-gel routes, namely: acid-catalyzed, basic catalyzed, acid, followed by basic catalysis (two steps) hydrolytic routes and a FeCl₃ catalyzed non-hydrolytic route. The extraction method (thermal, Soxhlet, water washing, ultrasound) was also evaluated. The resulting xerogels were characterized by porosimetry by the adsorption/desorption of nitrogen (BET method), Fourier-transform infrared spectroscopy (FTIR) and zeta potential. The preparation route did affect the textural properties of the materials. The best extraction capacity was achieved by acid and two-steps routes. Acid route showed the highest selectivity factor (2.5) between Rhodamine B and Rhodamine 6G. The best imprinting factor was achieved by the non-hydrolytic route. Competitive adsorptions were also carried out, resulting in an imprinting factor about 2. Apparently, the selectivity appears to be dictated by the shape generated through encapsulation and extraction rather than the magnitude of the surface area.

KEYWORDS: sol-gel; molecular-imprinting; silica.

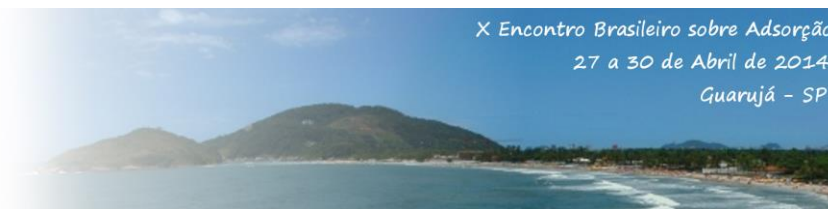
1. INTRODUCTION

Research on molecular imprinted (MI) materials has received much attention in the last years. Considering that such materials bear tailored-pore size and shape of the target molecule, these materials potentially bear high affinity and selectivity for the molecule employed as the template in the synthesis of the materials (Chen *et al.*, 2011). The molecular recognition ability of MI systems allows these materials to be used in processes such drug delivery (Cunliffe *et al.*, 2005), catalysis (Liu *et al.*, 2013), adsorption (Morais *et al.*, 2013), chemical sensing (Santos *et al.*, 2012), pre-concentration (Dai *et al.*, 2007), just to mention a few.

Concerning the development of molecular imprinted materials as sorbents for removal processes, the majority of the studies has reported the use of organic polymeric phases. Some drawbacks are associated with polymeric materials

such as the potential presence of functional chemical groups outside the printing sites, resulting in non-specific interactions and weak interactions between the *template* and polymer functional units, which in turn results in the leaching of the *template* during the early stages of polymerization. In addition, they may be characterized by low to moderate template recovery and heterogeneity of the produced receptor sites (Mayes & Whitcombe, 2005). One promising way to overcome some of these inconveniences is the use of inorganic matrices, such silica-based materials.

A potential approach to produce silica-based imprinted materials is by the sol-gel process. Briefly, this strategy consists in reacting the template with the precursor (e.g. tetraethylorthosilicate – TEOS), resulting in a silica network with the encapsulated molecule. Specific adsorptive sites are created after the removal of the template from silica network,



resulting materials with imprinted sites. According to the literature (Díaz-García & Laíño, 2005; Walcarius & Collison, 2009), these matrices prepared by the sol-gel method have some advantages in comparison with conventional organic polymerization methods, such as rigidity, thermal stability, tailored porosity, flexibility in processing conditions and the choice of monomers.

Regarding alcoxide-based silica materials some examples of the development of silica imprinted materials can be found in literature. For instance, acid route have been applied to synthesized molecularly imprinted xerogel to be used as sorbent for capillary microextraction using atrazine as a template and 3-(propylmethacrylate)trimethoxysilane as the precursor (Bagheri & Moghadam, 2012), for development of sensor for determination of trace olaquinox in chick feeds (Xu *et al*, 2012) and preparation of imprinted xerogel for the specific uptake of creatinine using tetraethoxysilane as the monomer precursor (Tsai & Syu, 2011). Acid and basic routes were investigated in the synthesis of glycylglycine-imprinted silica with potential application in selective chromatographic separation using tetramethoxysilane as the precursor (Ornelas, 2013). Likewise, basic route have been studied for applications such removal of cadmium(II) ions using CdCl_2 as molecule template and tetraethoxysilane as precursor (Wu & li, 2013). Non-hydrolytic materials were studied in combination with molecular imprinting for recognition of sulfonylurea herbicides using methacryloxypropyltrimethoxysilane as precursor (Si & Zhou, 2011). In addition, silicate-based materials have been applied for adsorptions of Au(III) using a solution of sodium silicate as the precursor and Au(III) as the template (Sakti *et al*, 2013).

The literature accounts for the capacity of interaction of organic molecules with titanium dioxide surfaces (Thomas & Syres, 2012). Combined with the concept of molecular imprinting, it may be expected a potential improvement in selective adsorption. Therefore, in the present manuscript, we report the preparation of a series of silica-based materials using TiCl_4 as Ti source prepared by different sol-gel processes, namely: hydrolytic (base and acid catalyzed), two steps (base, followed by acid catalysts) and non-hydrolytic route.

In the present study, we investigated the effect of different sol-gel routes on the adsorption

of Rhodamine B as the template molecule. In addition, textural and structural properties were also investigated. The effect of the extracting method (Thermal, Soxhlet, Washing, Ultrasound) was also evaluated.

2. EXPERIMENTAL SECTION

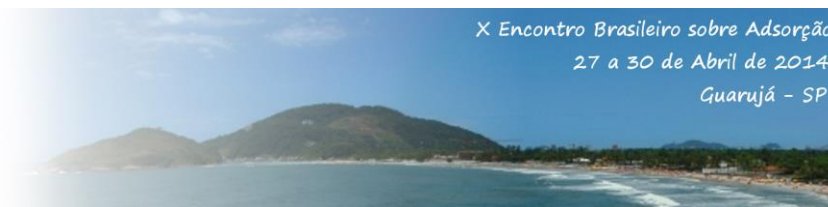
2.1. Materials and methods

Rhodamine B (Vetec), Rhodamine 6G (Sigma-Aldrich), tetraethoxysilane ($\text{Si}(\text{OCH}_2\text{CH}_3)_4$, TEOS, Merck, >98%), titanium tetrachloride (Merck, >99%) and silicon tetrachloride (SiCl_4 , Sigma-Aldrich, 99%) were used as received. Hydrochloric acid (HCl, Nuclear, 38%), ammonium hydroxide (NH_4OH , Nuclear, 29%) and FeCl_3 (98%, Merck) were employed as the catalysts.

2.2. Preparation of sol-gel materials

Five different routes were employed to prepare the samples by the sol-gel process using TEOS as the raw material. These were labeled as follows: acid catalyzed route 1 (A), acid catalyzed route 2 (A2), basic catalyzed route (B), two-steps route (TS) and non-hydrolytic route (NH). The acid route was catalyzed by 0.2 M of hydrochloric acid in a 1:2 (HCl:TEOS) ratio. The acid route 2 was quite similar, but the samples were prepared without the addition of hydrochloric acid (i.e., having TiCl_4 acting as a potential Lewis acid catalyst). The basic route was catalyzed by 0.2 M of ammonium hydroxide in a 1:2 (NH_4OH :TEOS) ratio. The two-steps route was catalyzed first by 0.2 M of hydrochloric acid in a 1:2 (HCl:TEOS) ratio and after 30 min., 0.2 M of ammonium hydroxide was added in a 1:2 (NH_4OH :TEOS) ratio. The non-hydrolytic route employed TEOS and SiCl_4 and was catalyzed by FeCl_3 (0.5 wt.-% of final product weight). For all samples the total amount of Rhodamine B (RhB) was fixed at 5 wt.-% of the final xerogel weight.

The samples (powder) obtained by acidic, basic and two-steps routes were prepared as follows: first, Rhodamine B was added into a solution of TEOS, then TiCl_4 , followed by the addition of the catalyst. During this process, the solution was kept under stirring at room temperature. The solution was stirred until gelation or until precipitation, which depends on the route.



For the non-hydrolytic route, all procedures were executed under inert atmosphere (Ar). Initially, the catalysts and Rhodamine B were added, followed by the addition of TEOS, SiCl_4 and TiCl_4 . The resulting solution was stirred at 80°C until gelation. All solids were dried at room temperature and then milled.

For template removal, several extraction methods were evaluated: thermal, Soxhlet, solvent washing and ultrasound. Thermal extraction was performed under Ar flow from room temperature up to 190°C at a heating rate of $5^\circ\text{C}/\text{min}$. Soxhlet extraction was employed in a suitable device using methanol as the solvent for 24 h. For ultrasound-assisted extraction, methanol and water were employed as solvent. The process was conducted altering modes of pulse on (20s) and pulse off (5s) during five minutes. For washing extraction water was used as the solvent. Finally, the solid was filtered and then dried at room temperature.

Thereafter, the resulting samples were labeled according to the sol-gel route. For example, NH stands for non-hydrolytic route. The use of TiCl_4 and the presence of encapsulated Rhodamine B were represented, respectively, by Ti and RhB. When necessary, E stands for systems with extractions. Therefore, ENHTiRhB refers to a xerogel prepared through the non-hydrolytic route that employed TiCl_4 during the synthesis and with Rhodamine B extracted. For comparative reasons, bare silica was also synthesized under the same conditions in the absence of the template. Thus, NH refers to a xerogel prepared through the non-hydrolytic route without TiCl_4 and Rhodamine B addition.

Figure 1 depicts the set of employed sol-gel routes and the corresponding resulting materials.

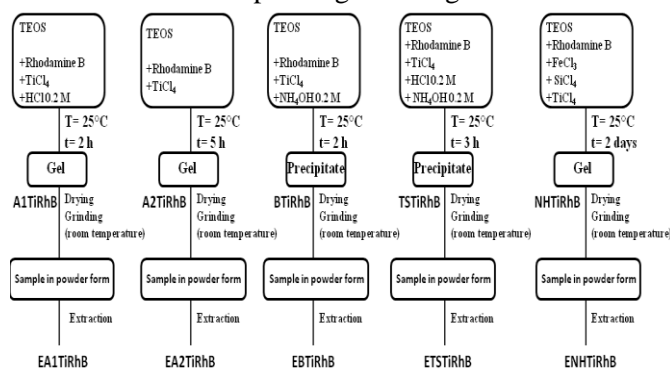


Figure 1. The different sol-gel routes employed for xerogel synthesis.

2.3 Xerogel Characterization

The specific surface area was determined by the Brunauer-Emmett-Teller (BET) method at -196°C , in the partial pressure range of $0.2 < P/P_0 < 0.9$. Samples were preheated at 110°C for 14 h under vacuum before each measurement. The total pore volume was obtained from single point desorption at $P/P_0 = 0.967$. The pore diameter was determined by Barret-Joyner-Halenda (BJH) method.

Fourier-transform infrared spectroscopy (FTIR) spectra were recorded at room temperature on a Bomem MB-102 Spectrometer by co-adding 36 scans with a resolution of 4 cm^{-1} .

The zeta potential of the xerogels (ca. 250 mg) was measured with a Zetamaster equipment (Malvern Instrument). Samples were dispersed in deionized water and then introduced into a closed capillary cell (DTS 1060).

2.4 Adsorption experiments

In a typical experiment, 10 mg of Rhodamine B-imprinted silica (extracted by ultrasound/methanol) were introduced into a cartridge, through which 5 mL of Rhodamine B solution ($\text{pH} = 5$) was percolated during 1 h. Similar experiments were done with the non-imprinted silica. Eluate was analyzed by UV-visible spectrometry at 553 nm. Adsorption (%) was calculated as $(C_{\text{final}} - C_{\text{initial}})/C_{\text{initial}} \times 100\%$. The imprinting factor, concerning the relative performance of the molecular-imprinted (MI)/non-imprinted (NI) pairs, was here defined as the MI:NI ratio of the concentration after the experiment.

In order to study the selectivity and competitive of the imprinted-materials, similar experiments were done with a solution of Rhodamine 6G. In this case, eluate was analyzed by UV-visible spectrometry at 525 nm. The selectivity factor was defined as the ratio between RhB and Rh6G adsorptions. In the case of tests of competitiveness, final concentration was calculated following the methodology described elsewhere (Connors & Eboka, 1979). All tests were performed in duplicate.



3. RESULTS AND DISCUSS

3.1 Characterization

The N_2 adsorption-desorption isotherms and the pore size distribution of A1TiRhB and EA1TiRhB are shown in Figure 2. According to Sing *et al* (1982) this profile is a typical characteristic for type IV isotherm: The adsorbed amount tends to a finite value, corresponding to

complete filling of the capillaries and type H2 hysteresis indicating that at the same relative pressure, the solid desorbs a smaller amount of adsorbed gas (Rouquerol *et al*, 1994). Moreover, taking into account the values of pore diameter (Table 1) it is possible to conclude that the resulting xerogels are mesoporous. It also can be noticed a narrow pore size distribution for both samples (insert in Figure 2), suggesting that the process of extraction did not affect the textural properties of this system.

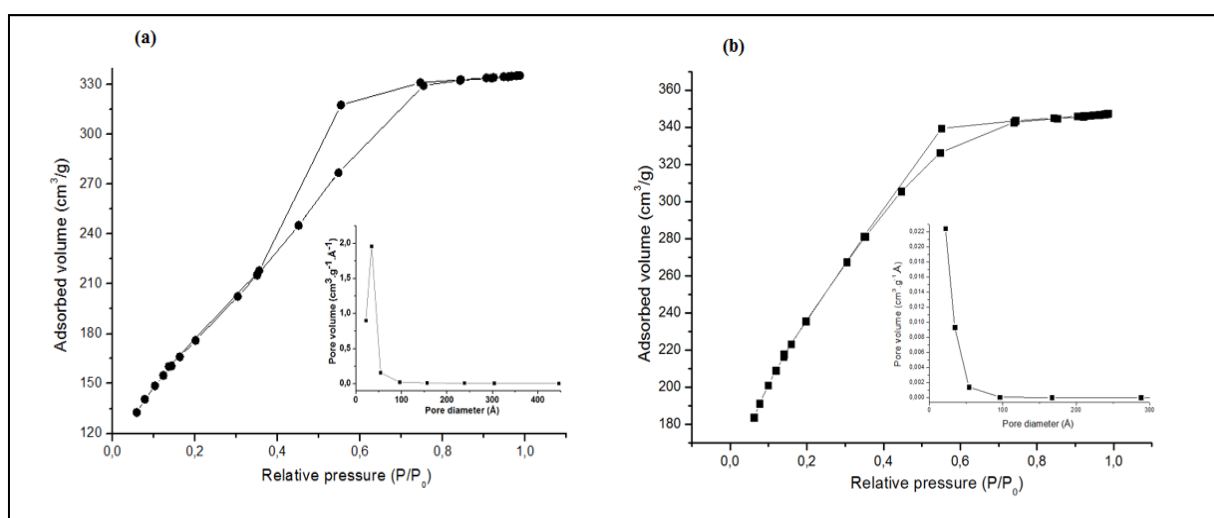


Figure 2. N_2 adsorption isotherm: (a) A1TiRhB, (b) EA1TiRhB. Insert: pore size distribution

Table 1. Textural parameters of the xerogels.

Route	S_{BET} (m^2/g)	V (cm^3/g)	D_p (Å)
A1	408	0.2	26.2
A1TiRhB (Thermal)	639	0.518	30.46
EA1TiRhB (Soxhlet metanol)	649	0.4	26.0
(Extraction method)	854	0.04	27.0
(Washing)	794	0.43	24.0
(Ultrasound water)	786	0.5	26.0
(Ultrasound methanol)	831	0.52	26.8
A2TiRhB	11	0.005	34.0
EA2TiRhB (Ultrasound methanol)	17	0.009	153.0
B	269	0.56	61.0
BTiRhB	511	0.3	26.0
EBTiRhB (Ultrasound methanol)	482	0.3	27.5
TS	373	0.18	23.0
TSTiRhB	568	0.5	29.0
ETSTiRhB (Ultrasound methanol)	350	0.13	30.0
NH	10	0.027	115.0
NHTiRhB	3	0.0044	48.0
ENHTiRhB (Ultrasound methanol)	31	0.014	28.0

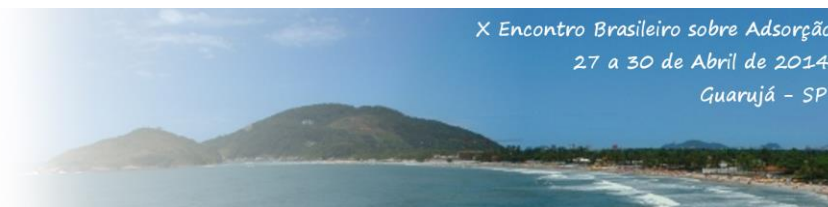
Comparing to A1TiRhB, similar patterns of isotherms and pore size distribution were obtained for TSTiRhB and NHTiRhB. Otherwise, A2TiRhB and BTiRhB showed a isotherm type I indicating

the presence of microporous materials with type H4 (shaped slit pores).

For some routes it was observed a changed of textural properties after extraction. For instance, EBTiRhB showed a typical characteristic of isotherm type IV with H2 hysteresis. As general trend, these results suggest that the preparation route did affect the textural properties of the materials.

According to Table 1, comparing the samples with encapsulated material with those without Rhodamine (for instance A1RiRhB and EA1TiRhB) it can be noticed an increase in surface area after its extraction. This fact indicates that the presence of dye perturbs the system, occluding the pores as previously reported in the literature (Munusamy *et al*, 2009).

The acid route (A1TiRhB) afforded the highest S_{BET} values, which are in agreement with the literature (Iler, 1979; Curran & Stiegman, 1999). Five extractions were employed for this system. Taking into account the BET surface area from the starting xerogel ($639 m^2 g^{-1}$), all the



extraction steps afforded an increasing in surface area, indicating the removal of the dye from the silica matrix. In other words, increasing the value of the area takes place after extraction, since the pores of silica, previously occupied by dye molecules, become free, and thus allow the adsorption of nitrogen. Therefore, it is reasonable to assume that the increase in surface area after extraction process results from the formation of cavities that produce an imprinted material. Nevertheless, the thermal extraction showed a small increase in surface area. As discussed by Limpo *et al* (1994), this result suggests that thermal treatment impinge a structure collapse of silica. On the other hand, extraction with ultrasound (methanol) showed the highest increase in the value of surface area estimated to be 854 m^2g^{-1} . The decrease in the value of the pore diameter also suggests the removal of dye molecules inside the silica network. Therefore, for all other samples the extractions were performed using ultrasound with methanol.

By analyzing the FT-IR spectra of the encapsulated systems (Figure 3 (a) and (c)) it can be noticed the main bands associated with Rhodamine B (Figure 3 Insert). It is worth noting that some bands, which are present in NHTiRhB, they are absent in A1TiRhB. For instance, the band at 1180 cm^{-1} , assigned to the asymmetric stretching of (C-O)-C (Liu *et al*, 2005), presenting in spectrum **a**, is absent after extraction (spectra **b**

and **d**) in Figure 3. Some of main bands of Rhodamine B showed wavenumber shifts. Table 2 summarizes the band shift for all systems with Rhodamine encapsulated. Excepting for the basic route (RBTiRhB), for all other systems were observed wavenumber shifts comparing the spectra of neat Rhodamine. Thus, this finding suggests a potential interaction of some groups from the dye structure with those of silica network. Regarding that that bands of the N-containing groups shifted in the spectra, a reasonable consequence is to considering the possibility of hydrogen bonding interaction between the dye and the silica via electron donation of these groups to the silica network (Morais *et al*, 2013).

For both BTiRhB and TSTiRhB a decrease in the value of surface area after the extraction is observed, and virtually no change in the value of the pore diameter (see Table 1). Conversely to the basic route, which no change was observed in the value of pore volume, the two steps route showed decreases in pore volume about 4 times lower. It is worth noting that in both routes, NaOH was employed as the catalyst. According to the literature (Brinker & Scherer, 1990), the sol-gel process in a basic pH results in materials with compact morphology. Thus, it is possible that the network of silica containing the dye was morphologically changed during the extraction process, resulting in a with pore volume.

Table 2. Main bands of the Rhodamine and attribution of band shift after encapsulation within silica framework

Neat Rhodamine		Encapsulated - Δu (cm^{-1})					Reference
Wavenumber (cm^{-1})	Assignment	Acid 1	Acid 2	Basic	Two Steps	Non-Hydrolytic	
1249	Stretch of C-N in -N (C_2H_5) ₂ group					-6	Liu et al 2005
1342	Asymmetric stretch of C-N-linked benzene ring and of C-O-C		-6			1	Liu et al 2005
1412	Bending of CH_2 in -N ⁺ (C_2H_5) ₂		-1		-10	1	Liu et al 2005
1529	Stretching modes of aromatic groups	-8	-2				Kerr et al 2013
1589	Stretch mode of C=C in benzene rings		1			1	Liu et al 2005
2870	Symmetric stretching of CH_3					-16	Wainippee et al 2010
2930	Antisymmetrical stretches of CH_2					5	Ereshchenko et al 1971
2979	Asymmetric stretches of CH_3					2	Wang & Lin 2005

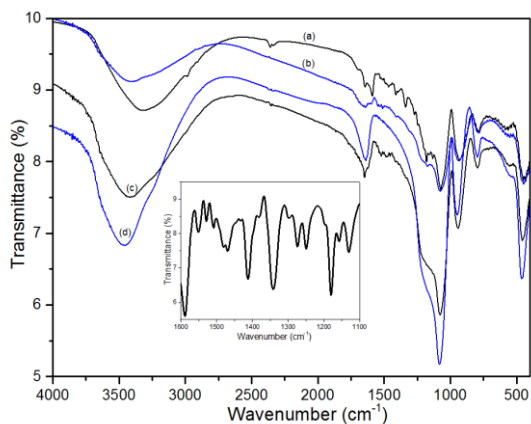


Figure 3. FT-IR spectra for encapsulated and extracted samples. (a) A1TiRhB, (b) NHTiRhB, (c) EA1TiRhB, (d) ENHTiRhB. Insert: FT-IR of Rhodamine between 1100 and 1600 cm^{-1} .

For the non-hydrolytic route an increase in the value of the specific area in more than 10 times after the extraction process was observed. In addition, pore volume exhibited an increase after extraction while pore diameter decreased 1.7 times. Thus, these results show an efficient extraction of the dye molecules within the silica network. Compared with other systems, NH showed the higher pore diameter. It is reasonable to assume that this behavior could have rendered easier the extraction of dye from the silica network.

3.1 Adsorption experiments

Selective adsorption of rodhamine B and Rhodamine 6G was carried out. Figure 4 shows the effect of route of the imprinted materials prepared by different sol-gel processes on selectivity. As a general trend, all imprinted material were able to remove selectively rodhamine B rather than rodhamine 6G. As shown in Table 2, the higher selectivity factor (SF) was achieved by the system ETSTiRhB (SF= 4) and the lower by the EA2TiRhB (SF= 2.1). These results suggest the capacity of silica for selective adsorption may be due the shape selectivity which certainly depends on the route of prepared xerogel. It is worth noting that for the system NH it can be noticed no appreciable difference of removal between the two dyes. These results show that the presence of porous, i.e., the system ENHTiRhB, not only allows higher values of removal but also a specificity of removal approximately of 1.8 times for Rhodamine B in comparison to Rhodamine 6G.

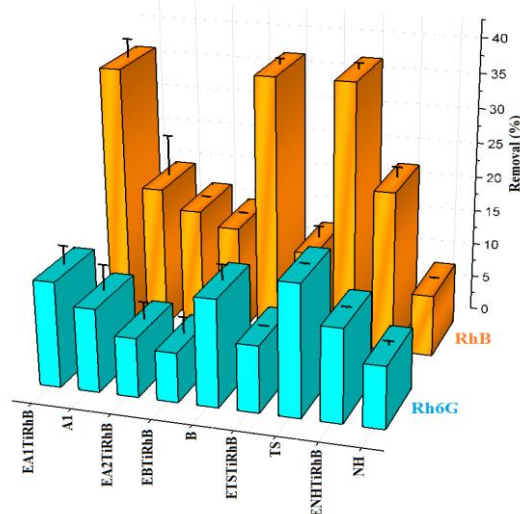


Figure 4. Influence of the sol-gel route on adsorption removal: selectivity tests.

Table 2. Maximum removal, imprinting factor, selectivity factor and zeta potential

System	Maximum removal RhB (%)	Maximum removal R6G (%)	Imprinting factor	Selectivity factor	Potential Zeta (mV)
EA1TiRhB	36.93	14.75	1.83	2.5	-11.9
EA2TiRhB	17.53	8.36	n.d.	2.1	13.1
EB1TiRhB	15.6	7	0.42	2.23	-12.6
ETSTiRhB	37.61	9.4	1.31	4.0	-8.99
ENHTiRhB	22.92	13.15	2.63	1.74	-14.9

As shown in Figure 4, it could be observed that imprinted xerogel possessed the highest adsorption capacity in comparison with the non-imprinted xerogel (bare silica). The systems EA1TiRhB and ENHTiRhB showed the highest imprinting factor (Table 2), which is evidence that imprinted xerogels possess specific binding sites for Rhodamine B. The only exception was the system EB1TiRhB that showed the lower removal of Rhodamine B and an imprinting factor equal to 0.4. One possible reason for this is due to leaching of molecules of Rhodamine from the interior of silica network during the adsorption process. As discussed above, this is in agreement with the decrease of area when compared with B1TiRhB (Table 1). Possibly, the extraction process was ineffective or the silica network was affected by the ultrasound process. Similar behavior was noticed for ETSTiRhB, even though the achieved imprinting factor was 1.3.

The values of potential zeta could also help explaining the value of maximum removal achieved by the systems. As seen in Table 2, the

potential zeta for those system is negative. According the literature (Garcia *et al*, 2005), Rhodamine B shows a positive charge bellow pH 6.0; therefore, the systems with negative zeta potential may have interact better with the dye. This is clearly evident the system EA2TiRhB, which showed positive potential zeta and aproximaty twice lower the value of maximum removal of Rhodamine B and Rhodamine 6G compared with EA1TiRhB. On the other hand, EBTiRhB also showed negative potential zeta and maximum removal similar to the EA2TiRhB. As previously discussed, this behavior may be due several reasons like leaching of molecules of Rhodamine from the interior of silica network, the lower surface area after the extraction and a formation of non specific sites of recognition of RhB.

Competitive adsorption of Rhodamine B by the imprinted sol-gel was also carried out with a mixture of Rhodamine 6G for the system EA1TiRhB and A1. From Figure 5 it can be noticed that system EA1TiRhB showed a removal of Rhodamine B 1.7 higher (27.21 %) than Rhodamine 6G (15.84 %). Thus, similarly to the selectivity tests, these results suggests that imprinted was successfully achieved within the network of silica. Moreover, the imprinting factor was about 2, which also indicates a much better binding ability for the imprinted sol-gel (EA1TiRhB).

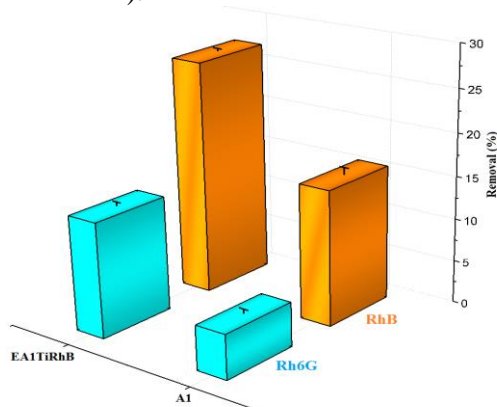


Figure 5. Influence of the sol-gel route on adsorption removal: competitive tests.

4. CONCLUSIONS

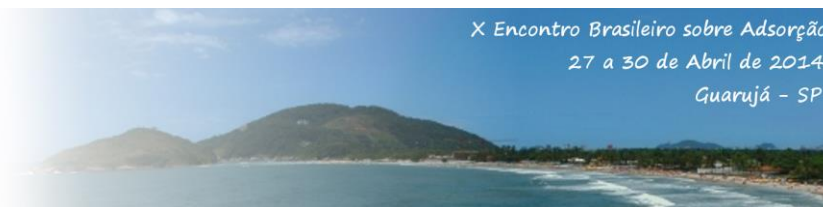
This study demonstrated that sol-gel route employed in the synthesis of imprinting materials can affect the textural characteristics of the

resulting xerogels, which in turn may affect the selective adsorption capacity. The preparation route did affect the textural properties of the materials, which is showed by different patterns of nitrogen adsorption isotherms depending on route as well as the high surface area value or systems in which were catalyzed by acid (acid and two-steps routes).

Among the investigated systems the non-hydrolytic route showed the highest increase in area after extraction, more than 10 times higher if compared with the encapsulated system (NHTiRhB). This result probably is correlated with the higher imprinting factor showed by this system (2.6). Higher values of surface area (EA1TiRhB and ETSiRhB) showed influences on the maximum removal of RhB. This trend seems to be related with more factors, once that the system EBTiRhB also resulted in an elevated value of surface area, though it showed the worst value of maximum removal of RhB. Moreover, the selectivity appears to be related more with the shape of network of silica obtained rather than the value of surface area.

4. REFERENCES

- BAGHERI, H.; PIRI-MOGHADAM, H. Sol-gel-based molecularly imprinted xerogel for capillary microextraction. *Anal. Bioanal. Chem.*, v. 404, p.1597-1602, 2012.
- BRINKER, C.J.; SCHERER, G.W. *Sol-Gel Science: The physics and chemistry of sol-gel processing*. Academic Press, 1990.
- CABRAL, C.; AZENHA, M.; SILVA, F. Synthesis of glycylglycine-imprinted silica microspheres through different water-in-oil emulsion techniques. *J. Chromatogr. A*, v. 1297, p.138-145, 2013.
- CHEN, L.; XU, S.; LI, J. Recent advances in molecular imprinting technology: current status, challenges and highlighted applications. *Chem. Soc. Rev.*, v. 40, p. 2922-2942. 2011.
- CONNORES, K.A.; EBOKA, C.J. Alternative graphical methods for the spectrophotometric analysis of mixtures. *Anal. Chem.*, v. 51, p. 1262-1266, 1979.
- CUNLIE, D.; KIRBY, A.; Alexander, C. Molecularly imprinted drug delivery systems. *Adv. Drug Deliv. Rev.*, v. 57, p. 1836-1853, 2005.



CURRAN, M.D.; STIEGMAN, A.E. Morphology and pore structure of silica xerogels made at low pH. *J. Non. Cryst. Solids*, v. 249, p. 62-68, 1999.

DAI, C.M.; GEISSEN, S.U.; ZHANG, Y.L.; ZHOU, X.F. Selective removal of diclofenac from contaminated water using molecularly imprinted polymer microspheres. *Environ. Pollut.*, v.159, p.1660-1666, 2011.

DÍAZ-GARCIA, M.E.; LAÍMÑO, R.B. Molecular Imprinting in Sol-Gel Materials: Recent Developments and Applications. *Microchim. Acta.*, v. 149, p.19-36, 2005.

GARCIA, A.; ISTA, L.K.; PETSEV, D.; O'BRIEN, M.K.; BISONG, P.; MAMMOLI, A.A.; BRUECK, S.R.J.; LÓPEZ, G.P. Electrokinetic molecular separation in nanoscale fluidic channels. *Lab. Chip.*, v. 5, p. 1271-1276, 2005.

ILER, R.K. *The chemistry of silica: solubility, polymerization, colloid and surface properties, and biochemistry*. Wiley, New York, 1979.

LIMPO, J.; BAUISTA, M.C.; RUBIO, J.; OTEO, J.L. Effect of heating on surface area and pore size distribution of monolithic silica gels. *Stud. Surf. Sci. Catal.*, v. 87, p.429-437, 19994.

LIU, X.; CUI, D.; WANG, Q.; XU, H.; LI, M. Photoluminescence enhancement of ZrO₂/Rhodamine B nanocomposites. *J. Mater. Sci.*, v. 40, p.1111-1114, 2005.

LIU, X.; LV, P.; YAO, G.; MA, C.; HUO, P.; YAN, Y. Microwave-assisted synthesis of selective degradation photocatalyst by surface molecular imprinting method for the degradation of tetracycline onto ClTiO₂. *Chem. Eng. J.*, v. 217 p. 398-406, 2013.

MAYES, A.G.; WHITCOMBE, M.J. Synthetic strategies for the generation of molecularly imprinted organic polymers. *Adv. Drug Deliv. Rev.*, v. 57, p. 742-1778, 2005.

SING, K.S.W. Reporting physisorption data for gas/solid systems with special reference to the determination of surface area and porosity. *Pure Appl. Chem.*, v. 54, p. 2201-2217, 1982.

MORAIS, E.C.; CORREA, C.G.; BRAMBILLA, R.; RADTKE, C.; BAIBICH, I.M.; DOS SANTOS, J.H.Z. The interaction of encapsulated pharmaceutical drugs with a silica matrix. *Colloid Surface B.*, v. 103, p.422-429, 2013.

MORAIS, E.C.; CORREA, G.G.; BRAMBILLA, R.; DOS SANTOS, J.H.Z.; FISCH,

A.G. Selective silica-based sorbent materials synthesized by molecular imprinting for adsorption of pharmaceuticals in aqueous matrices. *J. Sep. Sci.*, v.36, p. 636-643, 2013.

MUNUSAMY, P.; SELEEM, M.N.; ALQUBLAN, H.; TYLER, R.; SRIRANGANATHAN, N.; PICKRELL, G. Targeted drug delivery using silica xerogel systems to treat diseases due to intracellular pathogens. *Mater. Sci. Eng. C Mater. Biol. Appl.*, v. 29, p. 2313-2318, 2009.

ORNELAS, M.; LOUREIRO, D.; ARAÚJO, M.J.; MARQUES, E.; DIAS-THOMAS, A.G.; SYRES, K.L. Adsorption of organic molecules on rutile TiO₂ and anatase TiO₂ single crystal surfaces. *Chem. Soc. Rev.*, v. 41, p. 4207-4217, 2012.

ROUQUEROL, J.; AVNIR, D.; FAIRBRIDGE, C.W.; EVERETT, D.H.; HAYNES, D.H.; RAMSAY, J.D.F.; SING, K.S.W.; UNGER, K.K. Recommendations for the characterization of porous solids. *Pure Appl. Chem.*, v. 66, p. 739-1758, 1994.

SANTOS, W.J.R.; SANTHIAGO, M.; YOSHIDA, I.V.P.; KUBOTA, L.T. Electrochemical sensor based on imprinted sol-gel and nanomaterial for determination of caffeine. *Sens. Actuators B: Chem.*, v. 166-167, p.739-745, 2012.

TSAI, H.A.; SYU, M.J. Preparation of imprinted poly(tetraethoxysilanol) sol-gel for the specific uptake of creatinine. *Chem. Eng. J.*, v. 168, p.1369-1376, 2011.

WALCARIUS, A.; COLLISON, M.M. Analytical chemistry with silica sol-gels: traditional routes to new materials for chemical analysis. *Annu. Rev. Anal. Chem.*, v. 2, p. 121-143, 2009.

XU, Z.; SONG, J.; LI, L.; QIAO, X.; CHEN, H. Development of an on-line molecularly imprinted chemiluminescence sensor for determination of trace olaquinox in chick feeds. *J. Sci. Food Agric.*, v. 92, p. 2696-2702, 2012.

WAINIPWW, W.; WEISS, D.D.; SEPHTON, M.A.; COLES, B.J.; COURT, R. The effect of crude oil on arsenate adsorption on goethite. *Water Res.*, v. 44, p.5673-5683, 2010.

ERESHCHENKO, A.G.; STEPANTSOVA, N.P.; GELLER, B.E. Infrared spectroscopic study of the action of inorganic peroxides and gamma radiation on the arymethane dye rhodamine. *Appl. Spectros.*, v. 15, p. 1203-1206, 1971